INVESTIGATING THE IMPACT OF X-RAY COMPUTED TOMOGRAPHY IMAGING ON ORGANIC MATTER IN THE MURCHISON METEORITE: IMPLICATIONS FOR BENNU SAMPLE ANALYSES.

D. P. Glavin[1,*], C. M. O'D. Alexander[2], J. C. Aponte[1], A. A. Baczynski[3], E. L. Berger[4], A. S. Burton[4], G. D. Cody[2], J. P. Dworkin[1], S. A. Eckley[5], J. E. Elsila[1], F. T. Ferguson[1,9], D. I. Foustoukos[2], K. H. Freeman[3], Y. Furukawa[6], H. V. Graham[1], A. E. Hofmann[7], T. Koga[8], H. L. McLain[1,9], H. Naraoka[10], J. A. Nuth[1], Y. Oba[11], E. T. Parker[1], K. Righter[4], S. A. Sandford[12], P. Schmitt-Kopplin[13], D. N. Simkus[1,9], Y. Takano[8], H. C. Connolly Jr.[14,15], and D. S. Lauretta[15]. [1]NASA Goddard Space Flight Center (GSFC), Greenbelt, MD, USA, [2]Carnegie Institution for Science (CIS), Washington, DC, USA, [3]Penn State University, University Park, PA, USA, [4]NASA Johnson Space Center (JSC), Houston, TX, USA, [5]Jacobs, NASA JSC, Houston, TX, USA, [6]Tohoku University, Sendai, Japan, [7]Jet Propulsion Laboratory, California Institute of Technology, Pasadena, CA, USA, [8]JAMSTEC, Kanagawa, Japan, [9]Catholic University of America, Washington DC, USA, [10]Kyushu University, Fukuoka, Japan, [11]Hokkaido University, Sapporo, Hokkaido, Japan, [12]NASA Ames Research Center, Moffett Field, CA, USA, [13]Helmholtz-Zentrum Muenchen, Oberschleißheim, Germany, [14]Rowan University, Glassboro, NJ, USA, [15]Lunar and Planetary Laboratory, University of Arizona, Tucson, AZ, USA. [*]E-mail: daniel.p.glavin@nasa.gov.

Introduction: X-ray computed tomography (XCT) measurements are increasingly being used for 3D reconnaissance imaging of meteorites and returned samples to identify interesting lithologies or petrographic structures prior to sample processing and detailed mineralogical and chemical analyses [1]. Although XCT imaging is generally considered to be a non-destructive technique because silicate and metallic minerals in chondrites are not affected by X-rays at the intensities and wavelengths typically used, XCT can alter the natural radiation history of chondrites as measured by thermoluminescence [2]. Thus, there is also concern that XCT imaging could alter the organic content.

Previous experiments with the Murchison meteorite have shown that XCT and synchrotron XCT imaging up to a total dose of 2800 Gy do not alter the total amino acid abundances or their enantiomeric ratios in the meteorite after exposure [3,4]. However, the impact of XCT on bulk chemistry, other soluble organic matter (SOM) compound classes, and insoluble organic matter (IOM) in carbonaceous meteorites is unknown. To test this and inform planning for samples of carbonaceous asteroid Bennu being returned by the OSIRIS-REx mission, we conducted an XCT imaging experiment.

Samples and Methods: All glassware, ceramics, and sample handling tools used in this study were pyrolyzed at 500 ºC in air overnight. Multiple cm-sized chips of Murchison (USNM 5453) with a total mass of 10.3 g were hand crushed using a ceramic mortar and pestle. The powdered samples were not sieved in this study to reduce contamination risk. The powder was then transferred to a glass vial and homogenized by vortex mixing inside a positive pressure HEPA filtered laminar flow hood at JSC. Half of the total Murchison powder mass was transferred to a separate glass vial for use as a control and thus was not exposed to X-rays (labeled A). The remaining half (labeled B) was scanned using the Nikon XTH 320 CT instrument at NASA JSC (source energy: 160 kV; current: 38 μA; source to sample distance: 39.2 mm; duration: 500 min). A total X-ray dose of the sample of ~180 Gy during the scan calculated using the method of [4] represents the maximum dose a Bennu sample could experience during preliminary examination at JSC. Individual aliquots of the A and B powders were then sent to multiple institutions without revealing which sample had been in the XCT instrument as a "blind" test.

Both samples (~1.3 g each) were sent to the CIS for bulk C, N, and H abundance and isotopic analyses using an elemental analyzer-isotope ratio mass spectrometer (EA-IRMS) [5] and ^{1}H and ^{13}C solid state nuclear magnetic resonance (NMR) analyses of IOM residues isolated by CsF/HF acid dissolution of the meteorite powders [6]. NanoIR spectroscopy measurements of the IOM residues were also performed at the California State University San Marcos [7]. In addition, separate ~1 g portions of A and B were sent to Tohoku and Hokkaido Universities for the analyses of sugars [8] and N-heterocycles [9] in water and 2% HCl extracts using gas and liquid chromatography-mass spectrometry (GC-MS and LC-MS), respectively. ~2 g each of A and B were sent to GSFC to determine the distributions and abundances of other soluble organic compounds present in water and dichloromethane (DCM) extracts including protein amino acids, amines, aldehydes, ketones, monocarboxylic and hydroxy acids, alcohols, and polycyclic aromatic hydrocarbons (PAHs) using GC-MS and LC-MS [10]. The total surface areas of the A and B residues after water extraction were measured using a Quantachrome Nova 2200e analyzer at GSFC.

Results and Discussion: The XCT radiogram of B showed significant particle size heterogeneity with diameters up to ~1 to 2 mm for some grains. We report the bulk chemistry, SOM, and IOM data from the Murchison A and B samples. We assume that if there are no differences in the total abundances, distributions and isotopic compositions of organics in these samples

within analytical errors, then XCT has no impact on the sample. We did not determine the particle size frequency distribution of A, and given the range of particles sizes in B, SOM extraction efficiency differences between the samples must also be considered.

Bulk chemistry data. A summary of the average bulk C, N, and H abundances and their isotopic compositions from two replicate EA-IRMS measurements of ~20 mg of A and B is shown in Table 1. The data were similar within the 1-σ errors and are also consistent with previous analyses of Murchison [5]. They indicate that the A and B powders analyzed were chemically homogenous with respect to total C, N, and H with no evidence of alteration during the XCT scan.

Table 1. *Bulk chemistry data from the Murchison samples.*

Measurement	Control (A)	XCT (B)
Total C (wt.%)	1.92 ± 0.02	1.98 ± 0.03
Bulk δ^{13}C (‰)	-2.7 ± 0.1	-2.5 ± 0.5
Total N (wt.%)	0.101 ± 0.001	0.104 ± 0.002
Bulk δ^{15}N (‰)	+44.6 ± 0.2	+45.8 ± 0.8
Total H (wt.%)	1.058 ± 0.053	1.135 ± 0.057
Bulk δD (‰)	-33.2 ± 8.0	-38.9 ± 3.8

IOM data. Acid dissolution of the A and B powders yielded 16.4 and 18.1 mg of IOM, respectively, which represents ~1.5 wt.% of the total meteorite mass. ^{13}C and ^{1}H solid state NMR measurements of the IOM from A and B found that the fractions of aromatic C and aromatic H were identical and only slightly lower than the values previously measured for Murchison IOM [6]. These results show no impact from XCT on the molecular composition of IOM in Murchison.

SOM data. A comparison of the total abundances of targeted soluble organic compound classes measured in water (protein amino acids, amines, aldehydes, ketones, monocarboxylic and hydroxy acids, sugars, N-heterocycles) and DCM (alcohols, PAHs) extracts of ~0.5 to 1 g aliquots of the A and B powders is shown in Fig. 1. With the exception of alcohols and PAHs, the total abundances of all other soluble organic compound classes were higher in B than A, as indicated by the percentage change shown above the bars (Fig. 1). Despite these increases, there was no measurable change in the relative distributions of the individual compounds in each class after XCT. The very low sugar abundances measured in the A extract may be due to the higher Fe^{2+} concentration in the extract which required additional purification steps that were not done with the B extract and that could have led to additional analyte loss in A. Although the total abundance of pentoses in B was half that previously reported for another Murchison sample [8], the two comparative relative abundances were identical, indicating that X-rays did not alter the relative distribution of these sugars in B.

The ~20% increase in total amino acid abundances in B relative to A (Fig. 1) was surprising because previous experiments showed no change in amino acid abundances in Murchison after XCT imaging at even higher total X-ray doses [4]. The total surface area of the B residue after water extraction was slightly higher (22.8 ± 0.5 m^2/g) than the A residue (21.6 ± 0.6 m^2/g), which may explain the higher yields of protein amino acids and amines in B. It is also possible that the higher abundances of some soluble organics in B resulted from IOM breakdown by the X-rays during XCT.

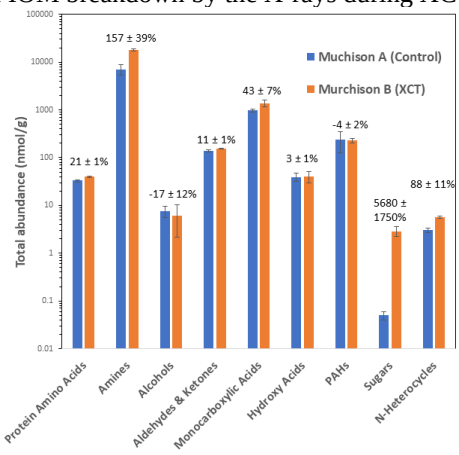

Figure 1. *Total abundances of soluble organics in the Murchison A (control) and B (XCT) samples. The percent abundance change from A to B is shown above the bars.*

Conclusions: XCT imaging of Murchison at a total X-ray dose of ~180 Gy had no effect on the bulk chemistry and average molecular composition of IOM within measurement errors and expected sample heterogeneity. The elevated abundances of most, but not all, SOM compound classes in B compared to A is likely related to surface area differences between the sample aliquots used for the extractions, rather than production from IOM by X-rays. Additional experiments will be needed to test this hypothesis. Nevertheless, these data provide confidence that XCT will not significantly alter the bulk chemistry and average molecular composition of IOM in samples returned by OSIRIS-REx.

References: [1] Ebel D. S. and Rivers M. L. (2007) *M&PS*, *42*, 1627-1646. [2] Sears D. W. G. et al. (2018) *M&PS*, *53*, 2624-2631. [3] Friedrich J. M. et al. (2016) *M&PS*, *51*, 429–437. [4] Friedrich J. M. et. al. (2019) *M&PS*, *54*, 220-228. [5] Alexander C. M. O'D. et al. (2012) *Science*, *337*, 721-723. [6] Cody G. D. and Alexander C. M. O'D. (2005) *GCA*, *69*, 1085-1097. [7] Gainsforth Z. et al. (2023) *LPS LIV*, this meeting. [8] Furukawa Y. et al. (2019) *PNAS*, *116*, 24440-24445. [9] Oba Y. et al. (2022) *Nat. Comm.*, *13*, 2008. [10] Aponte J. C. et al. (2020) *M&PS*, *55*, 1509-1524.

Acknowledgment: Work supported by NASA under Contract NNM10AA11C.